

Egyptian Crust: A structural modeling, based on gravity and seismic data

Ahmad Azab¹, Ali El-Khadragy² and Shokry A. Soliman¹

¹ Exploration Department, Egyptian Petroleum Research Institute, Cairo, Egypt

² Geology Department, Faculty of Science, Zagazig University, Zagazig, Egypt

shokry61@yahoo.com

Abstract: The present work depends essentially on the analysis of Bouguer gravity map constrained by the deep seismic data and geological information to reinterpret and delineate the regional crustal structure of Egypt. The approach intends first to evaluate the most efficient estimation of the crustal discontinuities depths. For that, the Bouguer gravity map was initially upwardly continued to proper heights and then the degree of regional polynomial to fit the Bouguer anomalies was done. As well, spectral analysis is used to estimate the approximate depths to the effective density interfaces of the crust, which serves as model data. At last, the evaluation of the structure of the crust has been accomplished through application of the 2D gravity modeling, based on the deep seismic refraction and spectral analysis results. The results indicate that, the complex gravity field of Egypt is attributed to different sources at varying depths of lithosphere. The Egyptian crust is essentially continental in type and suffers from lack of thickness at certain places. The northern and eastern margins exhibit thickness variations along marine boundaries, and density inhomogeneities within the crust or even the sub-crust. The crust-mantle boundary extended down to ~33Km below the Western Desert, with reduction in the thickness below Abu Gharadig basin (28km) and toward the Mediterranean Sea (~26km). Eastward, the Moho under the Eastern Desert is situated at depth of ~31Km, and significantly increases below the Red Sea hills (~37km). The results give evidence supporting a loss of the crust underneath the Gulf of Suez basin (~27km). The model across the northern Red Sea indicates the existence of oceanic crust below the main trough. The crustal thickness critically decreases beneath the axial zone (~11km). The sub-Moho reflector was roughly established at a depth of ~44km below the Egyptian shield, and was modeled at ~33km below the rift-axis.

[Ahmad Azab, Ali El-Khadragy and Shokry A. Soliman. **Egyptian Crust: A structural modeling, based on gravity and seismic data.** *J Am Sci* 2015;11(12):216-229]. (ISSN: 1545-1003). <http://www.jofamericansscience.org>. 28. doi:[10.7537/marsjas111215.28](https://doi.org/10.7537/marsjas111215.28).

Keywords: Egypt; Polynomial; Crustal structure; Sub-Moho; 2-D Modeling and Spectral Analysis.

1. Introduction

Egypt occupies the northeastern corner of Africa, between Latitudes 22° N&32°N and Longitudes 25°E&36°E (Fig.1). It covers about 10^6 Km² and forms part of a large belt extending from the Atlantic across the whole of North Africa.

In fact, the structure of Egyptian crust is a rather controversial problem, where the crust-mantle boundary remains unclear and sense speculative. The geometry of the crustal discontinuities is a key to understand the continental rifting and the initiation of sea floor spreading. In normal cases, the crust extends down to 30-35km below the continents, and is ~10km beneath sea level in the oceanic regions. This corresponds to a horizontal velocity discontinuity of 6.7-6.8 km/s, mapped below most regions of the African shield (**Ginzburg et al., 1979, Makris et al., 1979, Rehim, 1984 and Imam, 1988**). Below the zone of superficial rocks, the basement can be subdivided into two main layers; an upper crust of acidic (granitic/sialic) composition and lower crust probably of more basic (basaltic/mafic) nature. The boundary between these two layers, Conrad

discontinuity, cannot be easily recognized and is only known from seismic evidence (**Harris, 1971**).

Because of the uncertainties in the geometry and structure of the lower crust from deep seismic profiling, the crust have been revised and investigated by the method of gravity-seismic interpretation. The combined analysis may help to minimize existing uncertainties of the previous seismic experiments. The correlation between the seismic profiles and gravity data could help in estimation of the depths to crustal discontinuities.

The purpose of the study is to shed light on the deep crustal structure of Egypt from the gravity data and deep seismic profiles. The study concerns with the mass distribution and crustal configuration and their significant changes across the different tectonically interesting regions. The study focuses on the areal extent of Egyptian shield beneath the Red Sea and Mediterranean Sea to recognize the collision and diversion processes of the African plate with the Arabian and Eurasian plates and understanding the isostatic status of the area. For this purpose, a method proposed by Zeng (1989) was applied, where the distribution of the crustal discontinuities has been

approximated. The optimum degree of regional polynomial fitted to the Bouguer gravity data is estimated from the point of discontinuity of the gradient on a graph of variance against the polynomial degrees. This graph is obtained by means of fitting the polynomials of different degrees to an upward continuation of the Bouguer anomalies at a proper height, where the shapes of the anomalies are similar to those of the regional anomalies. The method may provide in-depth insight into the lithosphere. The spectral analysis was applied to estimate the average depths to the Conrad and Moho discontinuities, and basement surface. The technique executed on the

modeled profiles and the results were taken as a depth control. At last, the structure of the earth's crust was evaluated using the 2D gravity modeling along six profiles. The selected profiles occupy locations, where the shape of Moho discontinuity still remains a major key problem. The models go down into the lithosphere and disclose the shape/density variations at different interfaces. The modeling process used a number of deep seismic refraction profiles, as reference models and local constrains. Also, the tectonic map and geologic information were considered to accurate the model parameters.

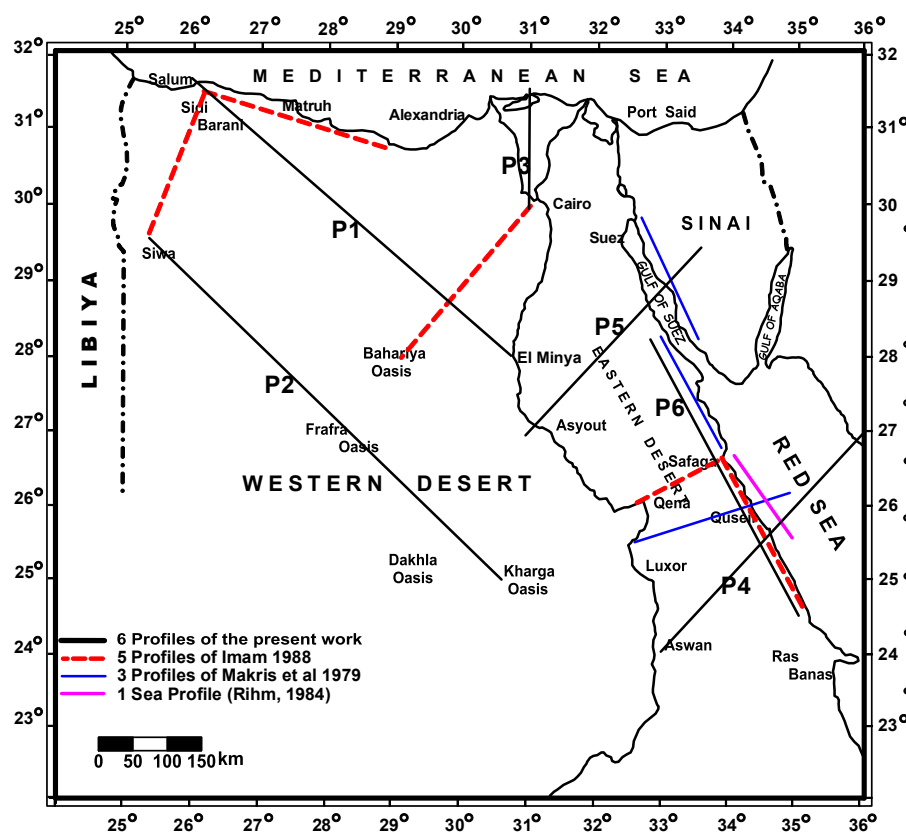


Fig. 1: Location map of the study area showing 2D modeling profiles

Geologic setting

Commonly, Egypt can be broadly divided into four structural divisions (Fig. 2), these are; Hing Zone and Unstable Shelf in the north, and the Stable Shelf and Nubian Craton in the south (Said, 1962). The main features of this map are segmented into three main provinces. The edge of the African Craton in Egypt represents the northern limit of the outcropping basement rocks in southern Egypt, Southern Sinai and the Red Sea Hills.

The Stable Shelf region represents the province that extends from the African Craton to the south and the Cretaceous shore-line to the north, which is

associated with ENE tectonic feature that cuts across Egypt through Gabel Dalma-Bahariya, uplift. The Unstable Shelf area is characterized by the Mesozoic to early Tertiary basins that separated from each other by ENE anticlinal folds. The extreme southern anticlinal fold is the Gabel Dalma-Bahariya uplift, which bounds the Abu Gharadig Basin and El Gindi Basin from the south. The basement tectonic map of Egypt (Meshref, 2002), as shown in Fig. 3, was guided to control the thickness variations of the sedimentary cover along the modeled profiles. It reflects the basins distribution and the chronological

sequence of tectonic events through the geologic times from pre-Cambrian to Recent.

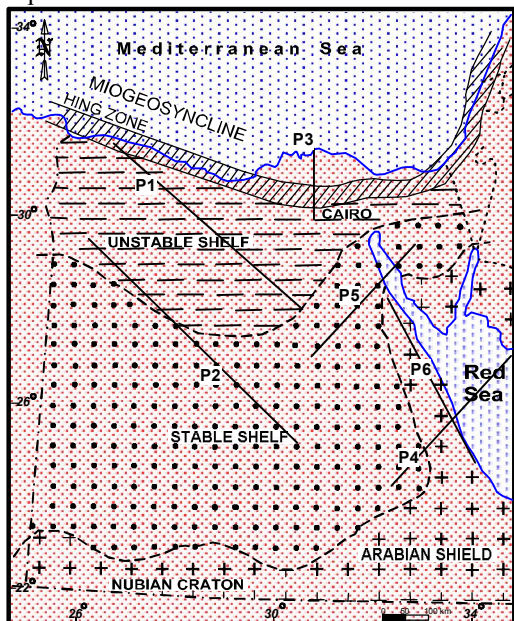


Fig. 2: Arabo-Nubian shield cratonic elements (after Said, 1962)

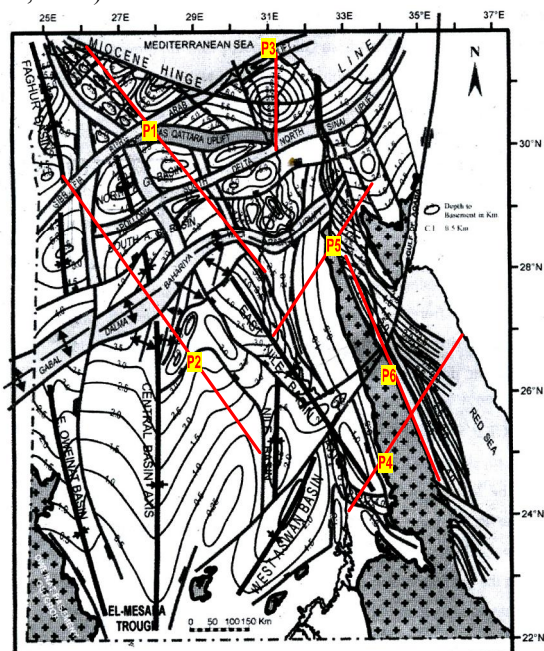


Fig. 3: Basement tectonic map of Egypt (after Meshref, 2002).

Bouguer map description

The gravity data are compiled from the Bouguer map of Egypt (General Petroleum Company, 1980). The Bouguer map (Fig. 4) shows great variations in the gravity field from the northwest to the southeast. It is generally defined by broad high and low gravity zones trending mainly in the ENE direction. Such fluctuations in the gravity field are associated with changes in the basement composition and depths, and reflect regional fold pattern. Close inspection of the Bouguer map shows that, the gravity field is characterized by relatively positive gravity signatures over the offshore areas, in contrast to negative ones over the onshore parts. For example, the Western Desert is described by broad negative gravity anomalies indicating that the crust-mantle boundary beneath the continental shield is much deeper. The southern portion (zone A), between Lats. 22° and 25°, where the sedimentary cover (Nubian Sandstone Fm.) became thinner, the gravity values range from 0 to -30 mGal. The central part (zone B) between Lat. 25° and 27° shows much lower gravity values ranging from -30 to -65 mGal. The northern portion (zone C) up to Lat. 29° is generally dominated by higher gravity anomalies varying from -30 to 0 mGal, associated with a thick sedimentary cover. The contours north of Lat. 30° (zone D) display a regional E-W high gravity trend (from 0 to ~70 mGal), with rapid increasing toward the Mediterranean Sea. Eastward, the Eastern Desert shows low gravity values ranging from 0 and -50 mGal. The negative anomalies became more extensive over the deep basinal areas. The gravity anomalies became less steeper over the Red Sea hills, (from 0 to -25 mGal), with a high relief toward the coastline. The northern part of the Red Sea (zone E) is well-defined by a strong NW-SE gravity trend, where the positive anomalies attain >85 mGal over its axis. Alternatively, both of the Gulf of Suez basin and the Gulf of Aqaba area show strong negative anomalies of about -70 & -100 mGal, respectively. The northern part of Sinai shows higher gravity values than the southern portion. The Delta basin exhibits relatively low gravity anomalies ranging between 0 and -35mGal.

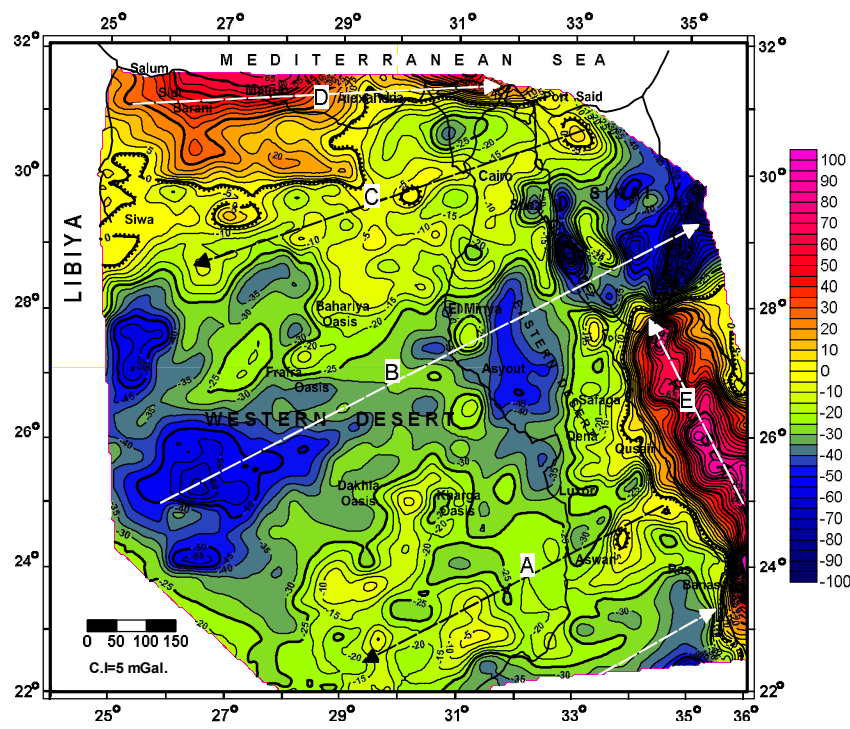


Fig. 4: Bouguer gravity map of Egypt (GPC, 1980).

Optimum polynomial fitting

Polynomial fitting by the least-squares is an effective method for the separation of gravity anomalies into residual and regional components. A review of the method was given by Nettleton (1976). However, the effectiveness of the method depends on selecting a proper order of regional to fit the gravity anomalies. The degree of the polynomial that gives the most efficient estimation of the trend from the Bouguer anomaly data was obtained by applying Zeng's technique (1989).

As is inferred from the geological and geophysical information, the Bouguer anomalies (ΔG_B) can be regarded as the superposition of anomalies reflected from three main density boundaries at varying depths, the Moho, Conrad and basement surfaces:

$$\Delta G_B = \Delta G_M + \Delta G_C + \Delta G_S$$

where: ΔG_M , ΔG_C & ΔG_S are the gravity anomalies due to Moho and Conrad discontinuities and basement respectively.

Our aim is to separate the regional anomalies of ΔG_C & ΔG_M at the observation planes from the Bouguer anomalies by means of fitting a regional polynomial of a proper order to the Bouguer map. First, we will evaluate the height H_c , where the anomalies at heights more than H_c are the single ones. So, the upward continuation of the Bouguer gravity (ΔG_B) to the heights of 5, 10, ..., 70 Km are evaluated successively and the number of extremal points (n),

i.e. the number of points with gradient $\partial \Delta G_B / \partial x, y = 0$ of each upward continuation contour map, is counted. According to Zeng (1989), the number (n) is considered as characteristic of the shape of the anomaly map. The obtained (n) values of the calculated upward continuation maps are plotted against the corresponding level, H (Fig. 5).

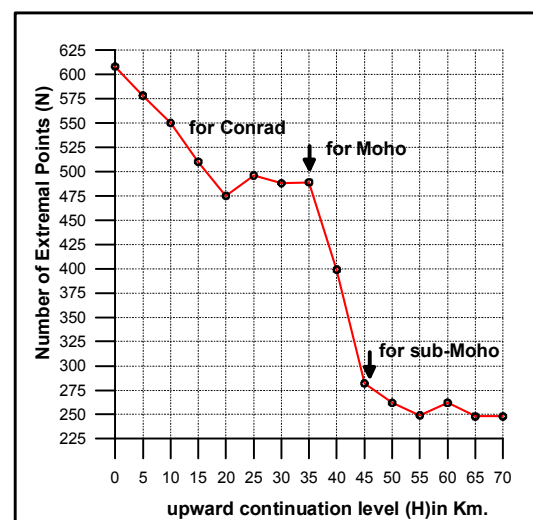


Fig. 5: Plot of the number of extremal points (N) against the upward continuation height (H) (5, 10, ..., 70 km)

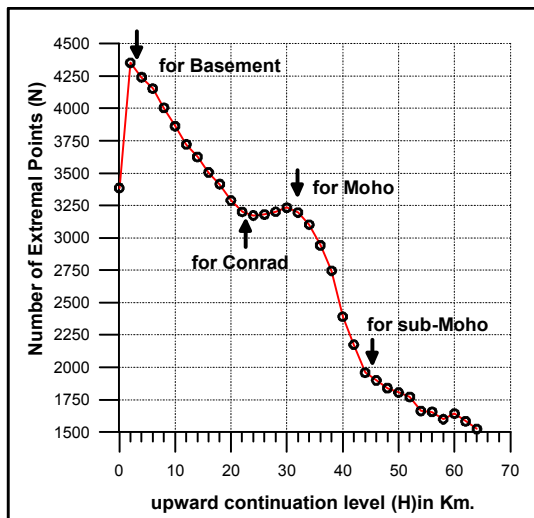


Fig.6: Plot of the number of extremal points (N) against the upward continuation height (H) (2,4,.....,64km)

From Fig.(5), it is seen that, for $H \geq 20$ Km, the number of extremal points (n) of the anomaly contour map at different heights is approximately constant. It shows that the anomalies at the heights equal to or greater than 20 Km are mainly single ones due to the Conrad discontinuity.

For more exactness, the Bouguer gravity anomalies (ΔG_B) are upwardly continued at 2,4,6,.....64Km, and the relation between the (n) values against (H) is constructed as shown in Fig.(6). It shows that, the anomalies at height 22 Km is the best fit for Conrad the discontinuity.

For comparison, the upward continued anomalies $\Delta G_{B(22)}$ at a height of 22 Km (Fig. 7) and the Bouguer anomalies show similar shape and configuration, although the upward continuations at a height above the observation level have strong attenuation in the magnitude.

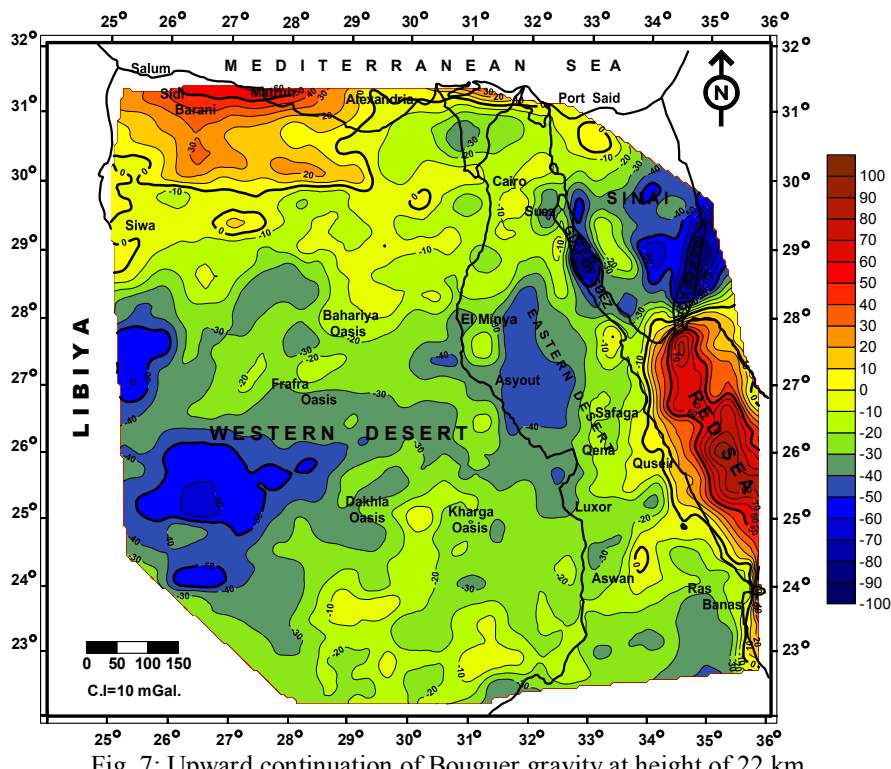


Fig. 7: Upward continuation of Bouguer gravity at height of 22 km.

Afterwards, the polynomials $P_d(x,y)$ of $d=1,2,.....,10$ have been fitted to the anomalies $\Delta G_{B(22)}$ and as a result, a graph of variance against the polynomial degree ($\sigma d - d$ characteristic) is constructed (Fig. 8).

The proper degree (d_n) of the regional polynomial could be estimated from the point of discontinuity of the gradient on this graph.

Accordingly, the optimum degree of polynomial representing $\Delta G_{B(22)}$ or ΔG_C is the fourth Fig. (8). As a result, the fourth degree of polynomial ΔG_{Reg4} represents the regional trend probably resulted from the Conrad discontinuity, has been fitted to the Bouguer anomalies ΔG_B . The residual anomalies ΔG_{Res4} Fig. (9), that associated with the upper crust (granitic basement), can be obtained by subtracting the

regional trend $\Delta G_{\text{Reg}4}$ from the Bouguer anomalies ΔG_B . They indicate that the complex gravity anomalies are surely linked with deep seated sources.

As shown before, the points of discontinuity at heights equal to 32 Km are considered to be due to the Moho discontinuity (Fig. 6). The proper order of polynomial fitting representing anomaly ΔG_M can be estimated by fitting the polynomials $P_d(x,y)(d=1,2,\dots,10)$ to the upwardly continued anomalies $\Delta G_{B(32)}$ (Fig. 10). The acceptable regional field and the residual field (Fig. 11) resulted from the Moho is represented by the gravity surface of the six order. It shows that, the degree of the polynomial adequately representing $\Delta G_{B(32)}$ or ΔG_M is $d=6$.

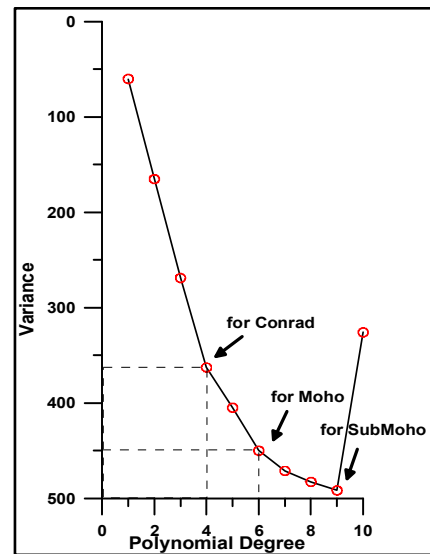


Fig. 8: Plot of the variance obtained from fitting polynomials $P_d(x,y)$ to the continuation field $G_B(22)$, against the polynomial degree(d)

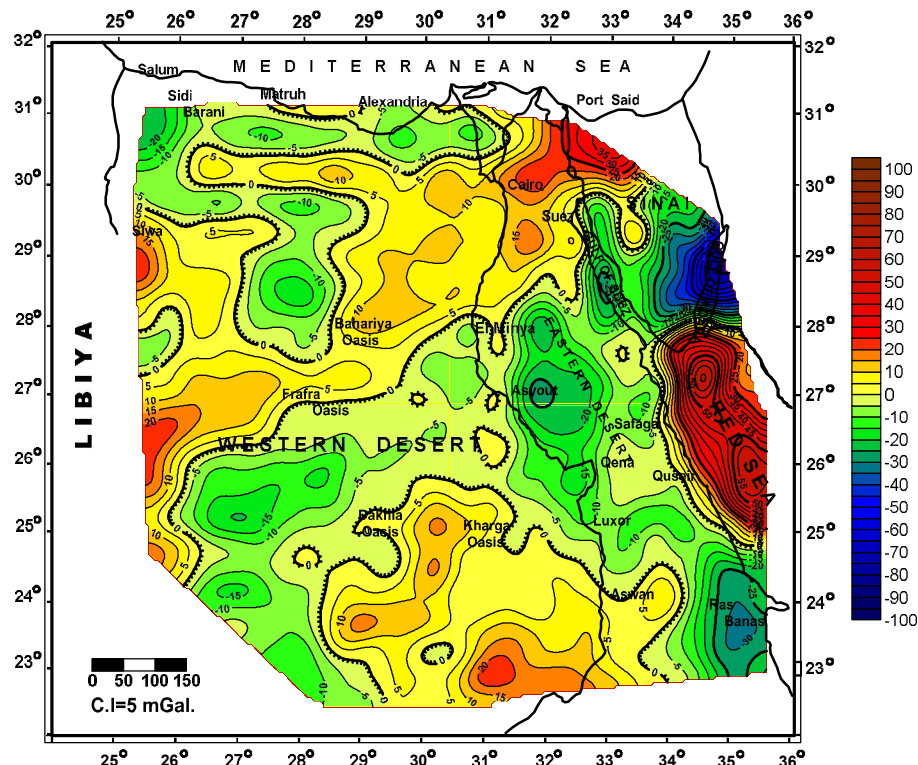


Fig. 9: Residual polynomial obtained in applying fourth degree fit to Bouguer gravity map

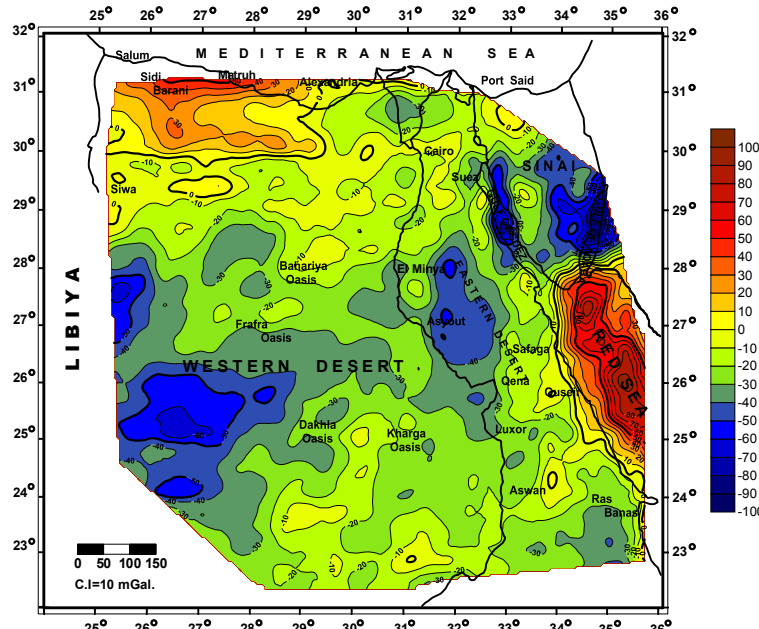


Fig. 10: Upward continuation of Bouguer gravity at high of 32km.

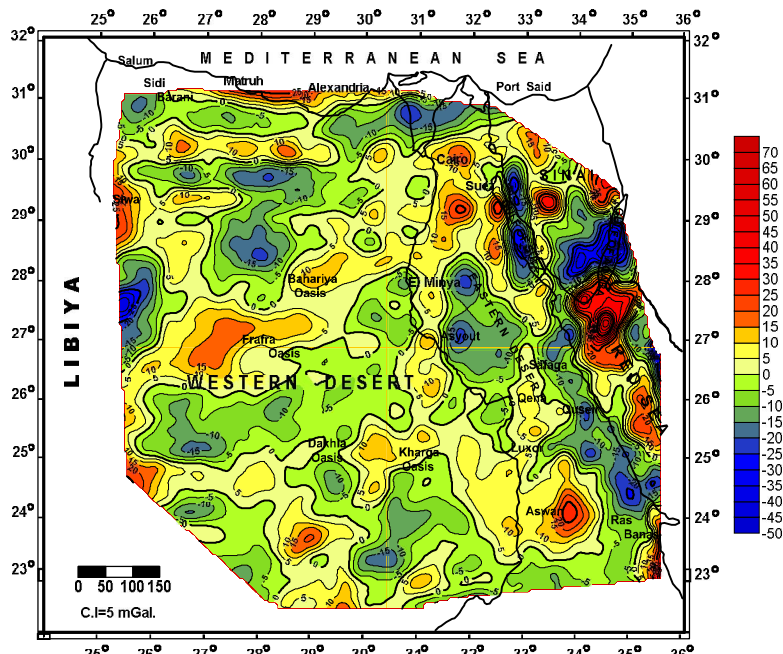


Fig. 11: Residual polynomial obtained in applying sixth degree fit to Bouguer gravity map

Furthermore, from)Fig.6(, we can conclude that, the depth of the sub-Moho discontinuity could be regarded as 44 Km beneath the continental crust. The accepted regional field for the sub-Moho can be obtained by applying the ninth-order of on the polynomial Bouguer map. Makris *et al.* (1979) found that, the sub-Moho reflector was clearly observed from the reflections and first arrivals along the Red Sea coast (Ras Benas-Safaga profile), giving Vp-

apparent velocity of 8.3 km/s at a depth of nearly 32 Km.

Spectral analysis

The radially average spectrum is used to obtain a rough estimate of depth to the crustal discontinuities. The practical depth limit is determined by the finite length of profile, which in practice means that the maximum depth that can be determined is at most about one-quarter or even one-fifth of the profile length (Sadek *et al.*, 1984). The technique was carried

out along the six modeled profiles (Fig.1). The power spectrum reveals that the gravity signals may be originated from different levels of depths. The results of the depth estimate (Table 1) indicate that the average depth to the "Moho" is between 25.6 and 37.8Km and for "Conrad" is about 17-22.5km. A representative sample from the obtained energy spectra are shown in Fig. 12.

Table 1: Depth estimation results of spectral frequency analysis for magnetic profiles

Profile No	Conrad Depth. (Km)	Moho Depth. (Km)
P1	17.3	34.3
P2	19.2	36.2
P3	22.5	32.5
P4	16.3	37.9
P5	11.1	30.1
P6	15.6	25.6

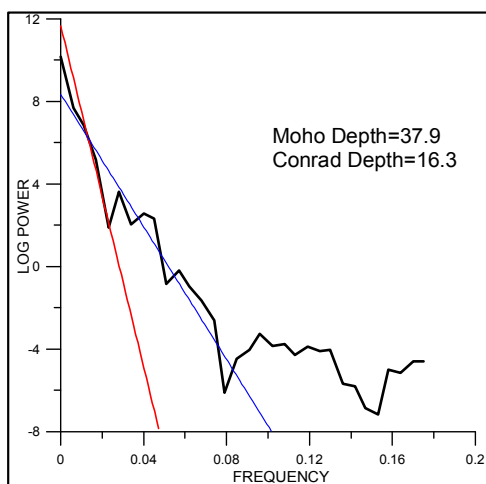


Fig. 12: Energy spectra of gravity data and the average depths calculated along profile (p4).

2D gravity models

In order to perform a quantitative interpretation for the subsurface structure, a simple 2D model approach was applied along six profiles P1- P6 (Fig. 1). Gravity modeling provides probable solutions on the subsurface depths, which can be considered as a good approximation to reality. The selected profiles traverse different structural parts and were taken, where the seismic refraction profiles were carried out. The density models become effective tool to judge investigate the crustal structure, particularly when combined with the geological and geophysical data. Thus, the depths to Conrad and Moho discontinuities are predicted from the integration of spectral analysis, as well as the deep seismic profiles (Makris *et al.*, 1979; Prodehl and Mechle, 1991; Rihm *et al.*, 1991). The densities of the crustal layers were obtained from previous works (Table 2). The thickness variations in the sedimentary section were roughly delineated using the basement depth map (Fig. 4).

The fitness between the observed and calculated profiles was accomplished using GM-Sys program (Geosoft, 1994). The calculated anomaly profile is matched with the corresponding observed one until get best fit from one iteration to another. The misfit between the observed and calculated values are partly due to the lack of constrain data.

Table 2: Density model and density correlation chart

Layers	Jacobs (1959)	Makris (1976)	Ginzburg (1987)	Abdel-Rahman <i>et al.</i> (1988)	Setto (1991)	Makris <i>et al.</i> , (1994)	Omran (1998)	Ismail (1998)	Omran <i>et al.</i> , (2001)	Azab (2009)
Sediments			2.50	2.45	2.46	2.36	2.3	2.4	2.37	2.42
U.Crust	2.67	2.82	2.80	2.68	2.68	2.82	2.67	2.70	2.67	2.78
L.Crust	3.00	2.90	2.96	2.9	2.90	2.90	3.00	3.10	3.07	2.93
U. Mantle	3.30	3.34	3.25		3.3	3.38	3.3	3.47	3.44	3.31

Salum-Elminya profile (P1)

Profile P1 (Fig. 13) cuts across the un table Shelf area and extends from Salum on the Mediterranean Sea coast to Elminya. It stretches in the NW-SE direction for about 460 Km through the topographic feature of the Qattara Depression. In general, the observed profile shows a progressive increase in the gravity values toward Salum. The basement surface is corrugated and varies from place to the other. Maximum thickness of the sediments reaches ~7km in

the Abu Gharadig basin and attains less than 3km at the Appolonia uplift. The pre-Cambrian basement complex is subdivided into upper ($d_u=2.75$ g/cc) and lower ($d_L=2.90$ g/cc) by the Conrad discontinuity, that run more or less parallel to the Moho at depths range from 17 to 21Km.

The northern portion is distinguished by a significant increase in the gravity values from 5 to 65 mGal. The high gravity gradient is explained by the

thinning of the continental crust, where the crust-mantle boundary decreased in depth from ~32Km below the Abu Gharadig basin to ~27Km at the Mediterranean coast.

The model shows that, the observed gravity minimum over Abu Gharadig basin is weak and not exceeds -20 mGal from the regional. In ordinary, a thick pile of sediments of 6-7km with a density contrast of ~0.43g/cc could cause a gravity anomaly not less than -110 mGal in magnitude. The difference

can be logically indicated by a dense source rock below the sedimentary section. The good fitting between the observed and the calculated gravity profiles was reached through making the Moho to be slightly thin below the deep basinal area. The model presumes that, Abu Gharadig feature represents a start point of a crustal thinning toward the north. The northern limit of the model is constrained by the Sidi Barrani-Sidi Abdelrahman profile and Matruh-Siwa profile (Makris, 1979).

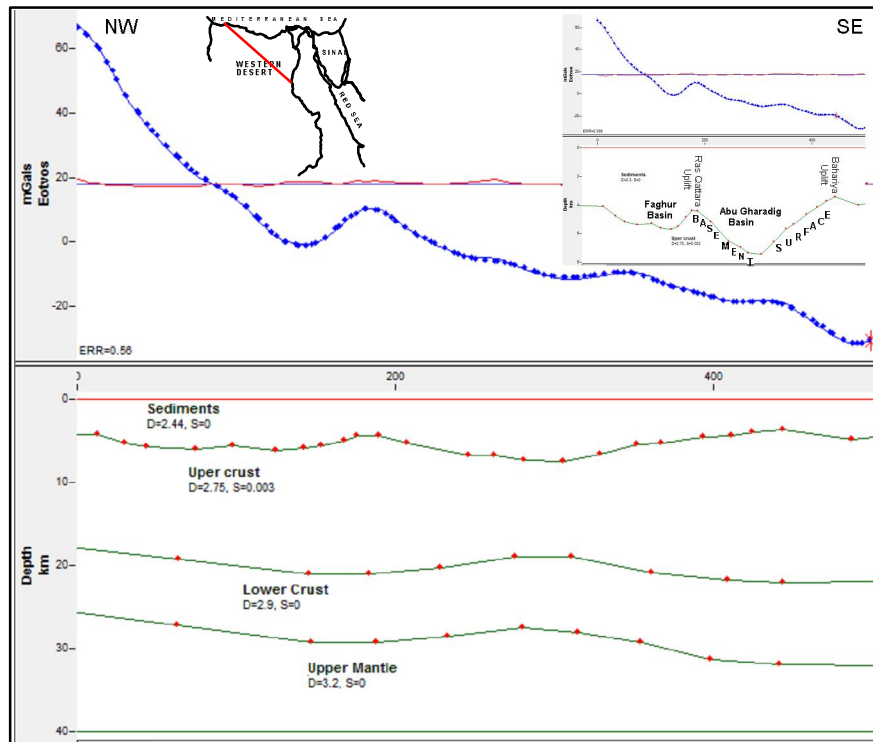


Fig. 13: 2-D gravity model along profile P1 (Salum-Elminya)

Siwa-Kharga Profile (P2)

Profile P2 (Fig. 14) transects from Siwa to Farafra to Kharga Oases, extending for ~810 km long. The model shows a normal continental crust with thickness of ~32km below the southern portion. To the north, the sedimentary section is underlain by thinner basement sections, and the Moho and Conrad are relatively shallower. The high gravity trend was interpreted to be due to decrease in the crust at depths from 30km to 27Km. The boundary between the two basement sections, is at a depth of 18-20 Km. The average densities of the upper and lower crust were assigned to be 2.75 g/cc and 2.90 g/cc, respectively, whereas the mean density of the upper mantle is 3.2 g/cc. The slope regime of the basement surface is

generally to the north, with thickening of the sediments in the prolific AG basin (>6km), which was confirmed by a large number of wells and seismic reflection sections.

As before, the model confirms a thin crustal thickness beneath AG basin, where the crust-mantle interface lies at shallow depth (~28km). Only dense source rocks are capable to compensate the negative gravity effect of such thick sedimentary section of AG basin. The proposed structure indicates that the intracontinental Qattara Depression occurs within a belt of thinned crust. The hypothesis was also proposed by Babeav, 1968, Imam (1991) Dorre, *et al.* (1997) and others.

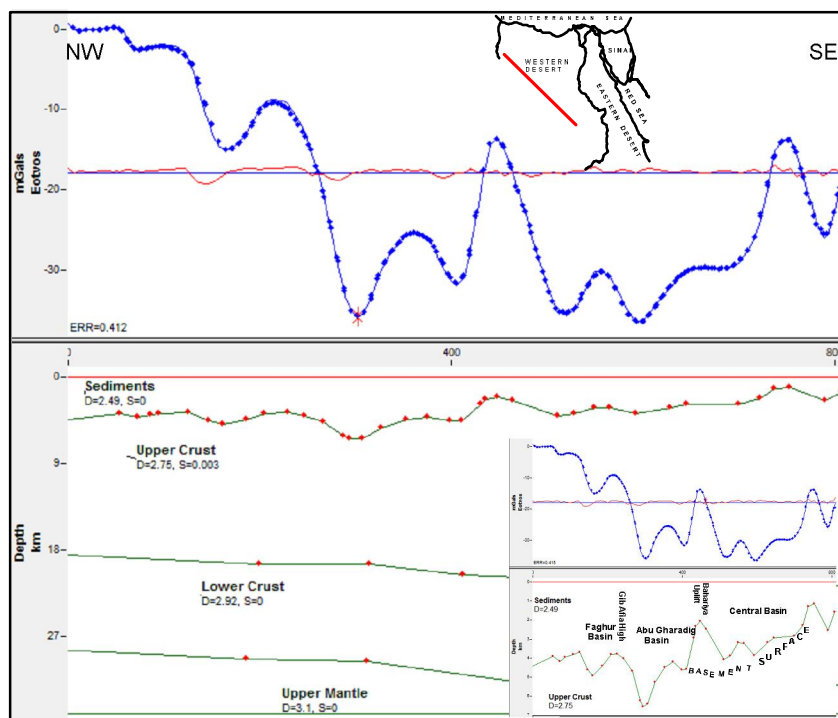


Fig. 14: 2-D gravity model along profile P2 (Siwa-Kharga)

Delta Profile (P3)

The profile extends vertically in the N-S direction across the delta, and spreads out for ~287Km long (Fig. 15). The model establishes a three density layers above the crust-mantle boundary. The low density sediments ($d_s=2.4$ g/cc) overlies two sections of basement rocks; the upper is of 2.75 g/cc and the lower is of 2.90 g/cc. The depth scale shows that, the average depths of the Conrad and Moho in the southern portion are ~22km & ~32km, respectively.

Visually, the northern portion of the profile is evidenced by a high gravity trend, that increases rapidly toward the sea (>65mGal). The depth to basement increase seaward (9-10 Km), and thicknesses of the sedimentary cover reache maximum at the foot of the continental margin. It is logic to assume a deep-seated source of high density contributing the regional gradient. The high gravity gradient (about 1mGal/km) is associated by unwrapping the Moho and wedging the basement rocks to the north. The negative gravity effect of the low density sediments is totally compensated by the positive effect of the high density upper-mantle materials. A correlation with Fig. 2 indicate that the Hing zone marks a zone of crustal transition between a typical continental crust below Egypt vis-à-vis a typical mafic crust below the Mediterranean sea. The southern portion of the model is seismically controlled by the Cairo-Bahariya refraction profile (Makris, 1979).

Aswan-Red Sea Profile (P4)

The profile extends in the northeastern direction, starts from Aswan and ends toward Saudi Arabia side (Fig. 16). It passes through the Eastern Desert, Red Sea hills and Red Sea geosyncline. The profile presents drastic changes in the thicknesses of crust from west to east. Westward, the crust below Aswan is ~32 km, and gradually increases to reach a maximum of ~37Km beneath the Red Sea Mountains. Along the Red Sea coast, the crust is still continental in type with reduction in thickness, which is some of ~22km. Away from the continental shelf, the crustal thickness decreases rapidly and minimize to ~11Km below the axial trough, before re-increasing underneath Saudi Arabia. The peak of the observed gravity profile is correlated with the maximum thinning of the oceanic crust.

Structurally, the oceanic crust is characterized by the absence of granitic basement. The low-density sediments ($d_s=2.4$ g/cc) are directly resting on the high density basement ($d_L=2.9$ g/cc) of the lower crust. The density of sea water ($d_w=1.033$ g/cc) was taken into consideration with the depth range is from 0 to 1000m.

The model evaluates the density distribution of the deep lithospheric structure of the Northern Red Sea rift. The density of the uppermost part of the mantle is relatively low (3.1 g/cc) if compared with the other profiles. This may support the possible presence of partial melting in the Northern Red Sea region. As well, the mass density of ~3.3 g/cc was

assigned for the base of the upper mantle, and the depth to the sub-Moho reflector is assumed to be at ~33km below the rift-axis. The sub-Moho reflector was seismically detected at a depth of ~32km below the sea level and a velocity of $V_p=8.3$ km/s (Makris *et al.*, 1979). As a result, the negative effect due to the

marine sediments (~5km) is isostatically compensated by the shallow dense mantle materials, as inferred from the strong positive gravity anomaly over the main trough. The subcrustal density is of significant effect on the fitting of the model and cannot be neglected.

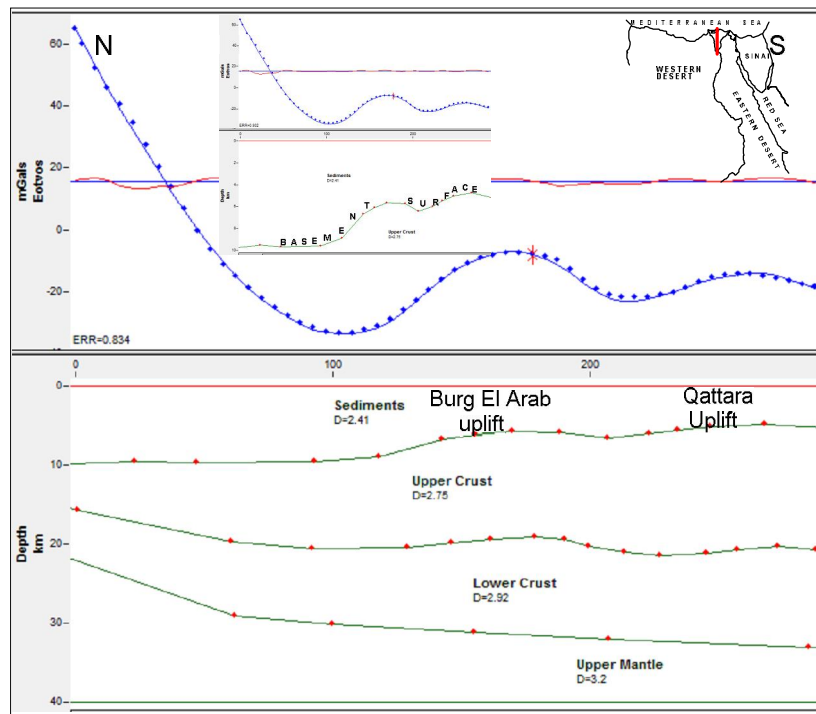


Fig. 15: 2-D gravity model along the profile P3 (Delta)

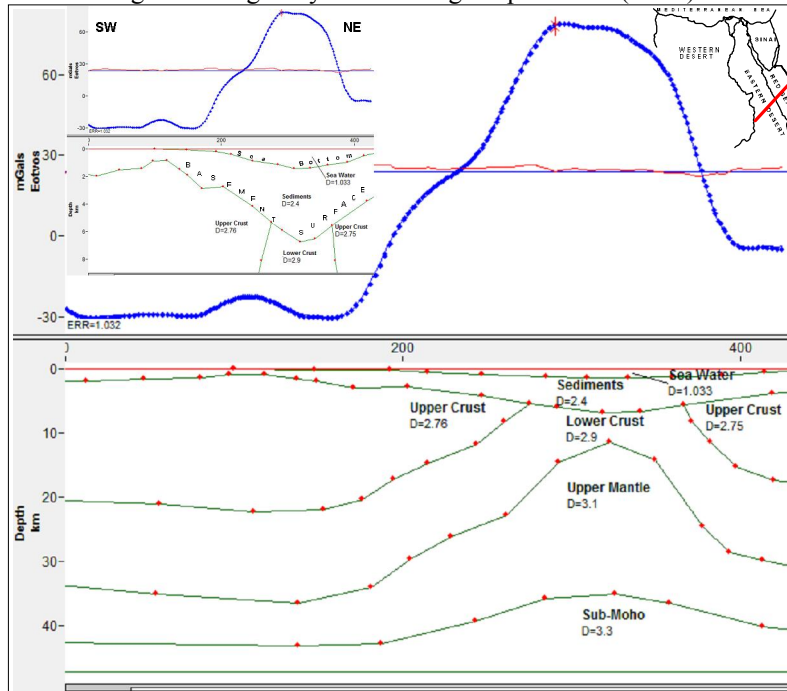


Fig. 16: 2-D gravity model along the profile P4 (Aswan-Red Sea)

Asuit–Sinai Profile (P5)

This transect P5 (Fig. 17) was modeled in the SW-NE direction, along a total length of ~470 km from Asuit to central Sinai. The western part of the model shows a normal crustal thickness of~32 km at Asuit that increases to reach a maximum depth of 35Km below the Galala Plateau. Over the Gulf of Suez, the observed gravity profile shows steep negative amplitude of -70 mGal. This gravity low is correlated with a thick sedimentary section (>6km) and with a density of 2.2-2.5 mGal. Such a thick pile

of sediments should result in a gravity effect not less than -110 mGal, which should be added to the mean value. The difference is considered to be due to deeper effect/source from the uppermost mantle. The good fitness is obtained by the thinning of crust below the main trough. The crust-mantle boundary is significantly reduced beneath the Gulf of Suez basin to be ~27Km. However, the negative amplitude indicate that the low gravity over the rift-basin is uncompensated completely by the mantle materials.

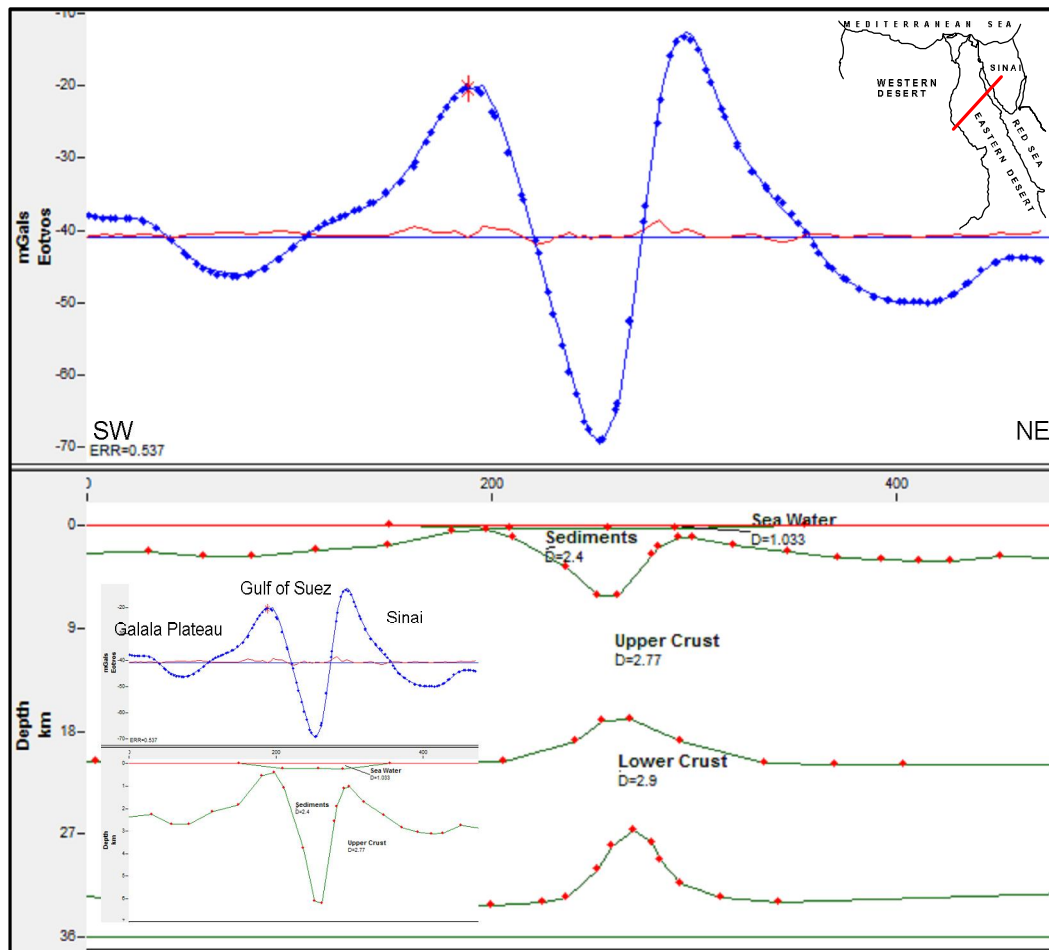


Fig. 17: 2-D gravity model along the profile P5 (Asuit -Sinai)

Red Sea Coast Profile (P6)

The profile p6 (Fig. 18) runs parallel to the Red Sea coastline, from the Suez in the north to Ras Banas in the south over a distance of ~470km. The profile lies along a boundary area of crustal stretching at the African Shield margin.

The proposed structure in the lower half indicates the presence of two-layered crust along the coastal plain. The Moho boundary seems to be featureless and lying at average depth of ~25 Km.

The granitic basement is separated from the basaltic basement at depths range from 12 to13 Km. Both of the Moho and Conrad discontinuities run in parallel style with slight northward dipping, associated with a regional gravity decrease. The gravity maxima are correlated with the shallow basement of the Red sea Mountain Ranges, while the minima are linked with the local basins. The crustal structure is matched with the deep seismic profiles of Makris (1979), and Imam (1988).

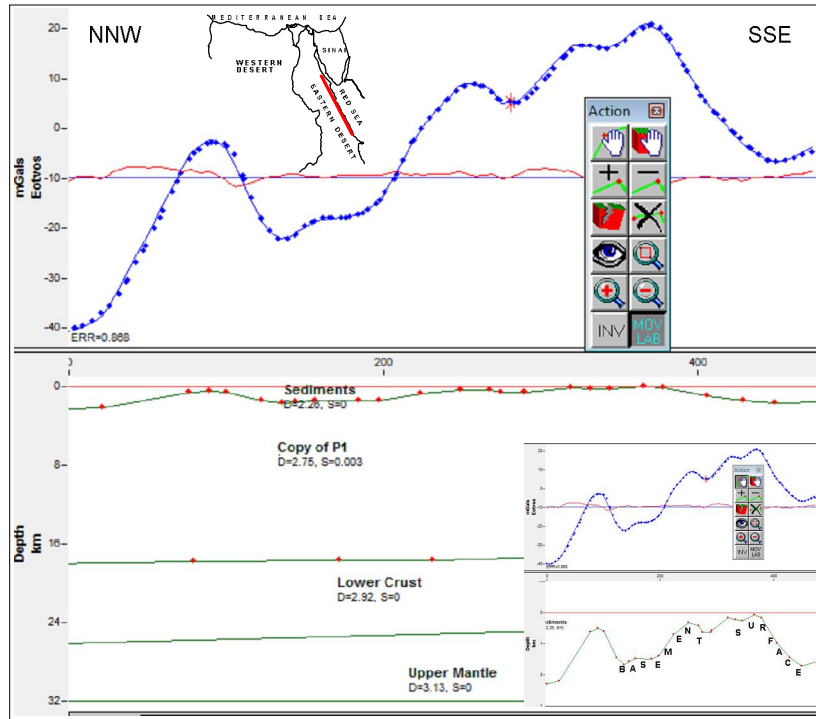


Fig. 18: 2-D gravity model along the profile P6 (Red Sea Coast)

Conclusions

- It is possible to conclude that, the gravity field of Egypt is composed of components due to deeper effect, such as changes in the thickness of crust and/or components resulting from structures on the basement and within the sedimentary cover.

- The models show a unchanged thickness of the crust below the Western Desert. The Nubian Craton, stable shelf and unstable shelf of Egypt have average thicknesses range between 31 and 33Km. Exceptionally, the crust below the Qattara depression suffers from lake, where the Moho lies at a depth of about 27km. The Hing zone confirms a rapid thinning of the crust toward the Mediterranean Sea (~26Km). The Arabian Craton exhibits a maximum thickening of the crust (about 37 Km) beneath the Red Sea hills. The crust below the main trough of the Red Sea is thin and reaches about 11 Km. Below the Gulf of Suez basin, the crus-mantle boundary is situated at depth of ~26 Km.

- The crust below the main trough of the northern Red Sea is totally oceanic and is nearly symmetrical in shape. Close association between the shape of the Moho and the regional gravity high may indicate a tendency for isostatic compensation.

- The results prove that, sub-Moho discontinuity can be known and defined in depth, not only from seismic, but also from gravity data. The approximate depth of the sub-Moho reflector, obtained from N-H plot (number of extremal points

against the upward continuation height) was calculated to be ~44km below the continental shield. The Red Sea profile indicates the sub-Moho discontinuity at a depth of ~33km below the rift-axis.

References

1. Abdel-Rahman, S.M., Refai, E.M., El-Ghalban, H.M., 1988. Gravity models of the Nile Delta Basin, Egypt. E. G. S. Proc. of 6th Ann. Mtg., 27-33.
2. Azab, A.A, 2009. An integrated study of potential and seismic methods on South Sitra area, Western Desert, Egypt. Ph.D Degree, Zagazig Univ., Faculty of Science, 300p.
3. Babaev, A. G. 1968. Oil and gas prospects of the U. A. R. Unpublished report, 18~. General Petroleum Company, Cairo.
4. Dorre, A. S., Carrara, E., Cella, F., Grimaldi, M., Hady, Y. A., Hassan, H., Rapolla, A. and Roberti, N., 1997. Crustal thickness of Egypt determined by gravity data. Journal of African Earth Sciences, 'Jot. 25. No. 3, PP. 425-434, 1997.
5. El Emam, A., 1990. The Agnes gravity/magnetic anomaly; implications for potential field geophysics in the Western Desert of Egypt. 10th EGPC Seminar, Cairo, Egypt, 13p.
6. General Petroleum company, 1980. Bouguer Map of Egypt, Project of Academy of Scientific Research and Technology, 1980.

7. Geosoft package, 1994 Geosoft mapping and processing system. Johannesburg, 17p.
8. Ginzburg, A., Ben Avraham, Z., 1987. The deep structure of the central and southern Levant continental margin. *Ann. Tectonicae* 1, 105-115.
9. Ginzburg, A., Makris, J., Fuchs, K., Perathoner, B., Prodehl, C., 1979. Detailed structure of the crust and upper mantle along Jordan Dead Sea rift. *Journ. Geophys. Res.* 84, 5605-5612.
10. Harris, P., 1971. The composition of the Earth in understanding the Earth. Artemis Press, Sussex, 53-70.
11. Imam, A.M., 1988. Study of crustal structure of Egypt deduced from deep seismic gravity profiles, Ph.D Degree, Hamburg University, Germany, 118p.
12. Ismail, M.A., 1998. Geophysical studies in northern part of Egypt. Ph.D. Thesis, Cairo Univ., 96p.
13. Jacobs, J.A., Russall, R.D., Tuzo, W.J., 1959. Physics and geology. McGraw-Hill, Toronto.
14. Makris, J., 1976. A dynamic model of the Hellenic Arc deduced from geophysical data. *Tectonophysics* 36, 339-346.
15. Makris, J., Weigel, W., Moller, L., Goldflam, P., Behle, A., Stofen, B., Allam, A., Maamoun, M., Delibasis, N., Perissoratis, K., Avedik, F., Giese, P., 1978. Deep seismic soundings in Egypt, part I: The Mediterranean Sea between Crete-Sidi Barrani and the coastal areas of Egypt (Unpublished).
16. Makris, J., Stofen, B., Vees, R., Allam, A., Maamoun, M., Shatta, W., 1979. Deep seismic sounding in Egypt. Part I, the Mediterranean Sea between Crete- sidi Barani and the coastal area of Egypt. Part II, crust and upper mantle of the Red Sea coast (unpublished).
17. Makris, J., Wang, S., Odintsov, D., Udintsov, G.B., 1994. The magnetic field of the eastern Mediterranean Sea, In Cruise 5 of the research vessel" Akademik Nikolaj Strakhov" Geolog. Survey of Isreal report, 87-98.
18. Meshref, W.M., 2002. Basement tectonic map of Egypt. Cairo 2002 international petroleum conference and inhabitation, Cairo, 1-5.
19. Mesko, A., 1984. Digital filtering. Applications in geophysical exploration for oil. John Wiely, New York, 298p.
20. Nettleton, I.I., 1976. Gravity and magnetic in oil prospecting. McGraw-Hill Book Com, 464p.
21. Omran, M.A., 1998. Structural evolution of Nile area, Egypt. *Jour. of Geology* 42, 1, 73-291.
22. Omran, M.A., Ismail, A., Selim, S., 2001. Crustal modeling of north Sinai and southeast Mediterranean Sea. *Proc. 2nd Internat., Symp. on Geophysics*, Tanta, 118-129.
23. Rihm, R., 1984. Seismische Messungen in Roten Meer und ihre interpretation. Diplom Arbeit fur Geophysik der universitat Hamburg, 1984.
24. Sadek, H.S., Rashad, S.M., Blank, H.R., 1984. Spectral analysis of aeromagnetic profiles for depth estimation, principles software and practical application. Ministry of petroleum and Min. Res. Saudi Arabia. Report USGS-OF-o4-27(IR 656). 40p.
25. Said, R., 1962. The geology of Egypt. Elsever Pub!. Co, Amsterdam.
26. Setto, I.A., 1991. A crustal model for the Nile Delta, Egypt. *J. Geol.* 34 (1-2), 279-292.
27. Zeng, H., 1989. Estimation of the degree of polynomial fitted to gravity anomalies and its application. *Geophysical prospecting*, 37, 959-973.

12/25/2015